

A NOVEL SUPER-CAPACITOR ENERGY STORAGE OF DFIG WIND TURBINES WITH AN ADVANCED FUZZY LOGIC CONTROLLER

Kilari Gangadhar¹, T.Venkatesh², P.Purna Chandrarao³

¹M.Tech (PSC & AE) Student Department Of EEE, Chalapathi Institute Of Technology

² Asst. Professor, Department Of EEE, Chalapathi Institute Of Technology Mothadaka

³Head Of The Department Of EEE, Chalapathi Institute Of Technology Mothadaka

ABSTRACT:

With the increasing penetration of wind power into electric power grids, energy storage devices will be required to dynamically match the intermittency of wind energy. This paper proposes a novel two-layer constant power control scheme for a wind farm equipped with doubly fed induction generator (DFIG) wind turbines with FUZZY control. Each DFIG wind turbine is equipped with a super capacitor energy storage system (ESS) and is controlled by the low-layer wind turbine generator (WTG) controllers and coordinated by a high-layer wind farm supervisory controller (WFSC). The WFSC generates the active power references for the low-layer WTG controllers according to the active power demand from or generation commitment to the grid operator; the low-layer WTG controllers then regulate each DFIG wind turbine to generate the desired amount of active power, where the deviations between the available wind energy input and desired active power output are compensated by the ESS with FUZZY controller. Simulation studies are carried out in MATLAB on a wind farm equipped with 15 DFIG wind turbines to verify the effectiveness of the proposed control scheme.

I. INTRODUCTION:

WIND TURBINE generators (WTGs) are usually controlled to generate maximum electrical power from wind under normal wind conditions. However, because of the variations of the wind speed, the generated electrical power of a WTG is usually fluctuated. Currently, wind energy only provides about 1%–2% of the U.S.'s electricity supply. At such a penetration

level, it is not necessary to require WTGs to participate in automatic generation control, unit commitment, or frequency regulation. However, it is reasonable to expect that wind power will be capable of becoming a major contributor to the nation's and world's electricity supply over the next three decades. For instance, the European Wind Energy Association has set a target to satisfy more than 22% of European electricity

demand with wind power by 2030 [1]. In the U.S., according to a report [2] by the Department of Energy, it is feasible to supply 20% of the nation's electricity from wind by 2030. At such high levels of penetration, it will become necessary to require WTGs to supply a desired amount of active power to participate in automatic generation control or frequency regulation of the grid [3]. However, the intermittency of wind resources can cause high rates of change (ramps) in power generation [4], which is a critical issue for balancing power systems. Moreover, to optimize the economic performance of power systems with high penetrations of wind power, it would be desired to require WTGs to participate in unit commitment, economic dispatch, or electricity market operation [5]. In practice, short-term wind power prediction [6] is carried out to help WTGs provide these functions. However, even using the state-of-the-art methods, prediction errors are present [5]. Under these conditions, the replacement power is supported by reserves, which, however, can be more expensive than base electricity prices [7].

This paper proposes a novel two-layer constant power control (CPC) scheme for a wind farm equipped with doubly fed induction generator (DFIG) wind turbines [14], where each WTG is equipped with a supercapacitor energy storage system (ESS). The CPC consists of a high-layer wind farm supervisory controller (WFSC) and low-

layer WTG controllers. The highlayer WFSC generates the active power references for the lowlayer WTG controllers of each DFIG wind turbine according to the active power demand from the grid operator. The low-layer WTG controllers then regulate each DFIG wind turbine to generate the desired amount of active power, where the deviations between the available wind energy input and desired active power output are compensated by the ESS. Simulation studies are carried out in PSCAD/EMTDC for a wind farm equipped with 15 DFIG wind turbines to verify the effectiveness of the proposed control scheme.

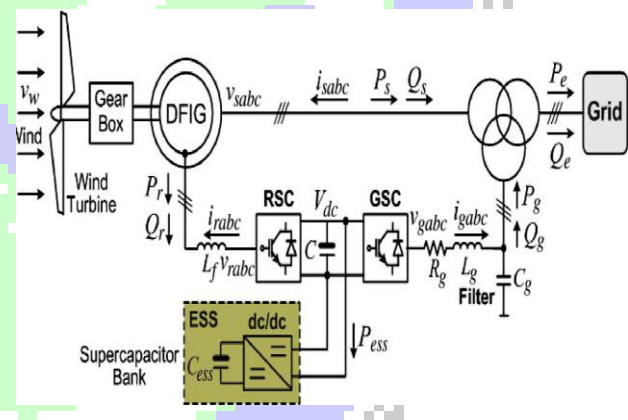


Fig. 1. Configuration of a DFIG wind turbine equipped with a supercapacitor ESS connected to a power grid

II. DFIG WIND TURBINE WITH ENERGY STORAGE

Fig. 1 shows the basic configuration of a DFIG wind turbine equipped with a supercapacitor-based ESS. The low speed

wind turbine drives a high-speed DFIG through a gearbox. The DFIG is a wound-rotor induction machine. It is connected to the power grid at both stator and rotor terminals. The stator is directly connected to the grid, while the rotor is fed through a variable-frequency converter, which consists of a rotor-side converter (RSC) and a grid-side converter (GSC) connected back to back through a dc link and usually has a rating of a fraction (25%–30%) of the DFIG nominal power. As a consequence, the WTG can operate with the rotational speed in a range of $\pm 25\%$ –30% around the synchronous speed, and its active and reactive powers can be controlled independently. In this paper, an ESS consisting of a supercapacitor bank and a two-quadrant dc/dc converter is connected to the dc link of the DFIG converters. The ESS serves as either a source or a sink of active power and therefore contributes to control the generated active power of the WTG. The value of the capacitance of the supercapacitor bank can be determined by

$$C_{ess} = \frac{2P_n T}{V_{sc}^2} \quad (1)$$

where C_{ess} is in farads, P_n is the rated power of the DFIG in watts, V_{sc} is the rated voltage of the supercapacitor bank in volts, and T is the desired time period in seconds that the ESS can supply/store energy at the rated power (P_n) of the DFIG. The use of an ESS in each WTG rather than a large single central ESS for the entire wind farm is based on two reasons. First, this

arrangement has a high reliability because the failure of a single ESS unit does not affect the ESS units in other WTGs. Second, the use of an ESS in each WTG can reinforce the dc bus of the DFIG converters during transients, thereby enhancing the low-voltage ride through capability of the WTG [10].

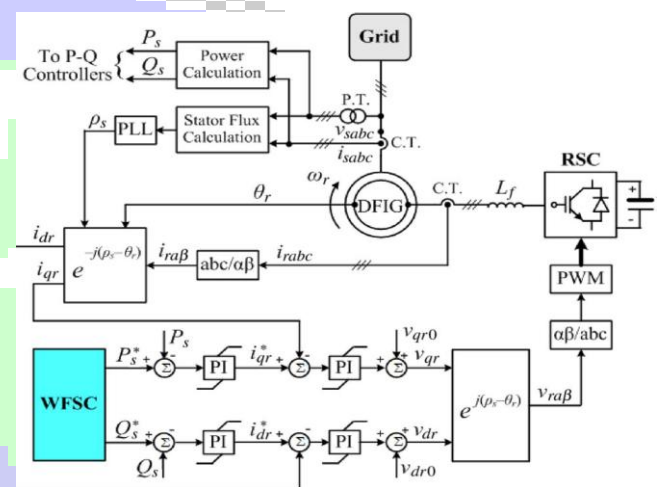


Fig. 2. Overall vector control scheme of the RSC.

III. CONTROL OF INDIVIDUAL DFIG WIND TURBINE

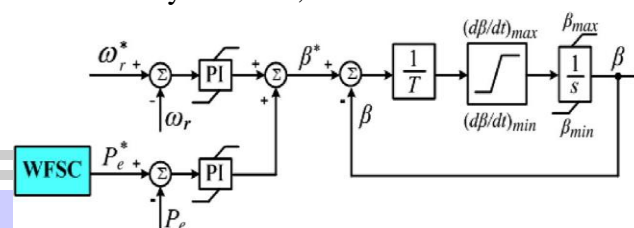
The control system of each individual DFIG wind turbine generally consists of two parts: 1) the electrical control of the DFIG and 2) the mechanical control of the wind turbine blade pitch angle [14], [15] and yaw system. Control of the DFIG is achieved by controlling the RSC, the GSC, and the ESS (see Fig. 1). The control objective of the RSC is to regulate the stator-side active power P_s and reactive power Q_s

[illegible]

Fig. 3. Overall vector control scheme of the GSC.

Fig. 3 shows the overall vector control scheme of the GSC, in which the control of the dc-link voltage V_{dc} and the reactive power Q_g exchanged between the GSC and the grid is achieved by means of current regulation in a synchronously rotating reference frame [16]. Again, the overall GSC control scheme consists of two cascaded control loops. The outer control loop regulates the dc-link voltage V_{dc} and the reactive power Q_g , respectively, which generates the reference signals i^*_{dg} and i^*_{qg} of the d- and q-axis current components,

0.5, where $V_{SC,n}$ and $V_{dc,n}$ are the nominal voltages of the supercapacitor bank and the DFIC dc link, respectively. Therefore, the nominal duty ratio $D_{1,n}$ of S1 is 0.5.



C. Configuration and Control of the ESS

The operating modes and duty ratios $D1$ and $D2$ of the dc/dc converter are controlled depending on the relationship between the active powers P_r of the RSC and P_g of the GSC. If P_r is greater than P_g , the converter is in buck mode and $D1$ is controlled, such that the supercapacitor bank serves as a sink to absorb active power, which results in the increase of its voltage V_{SC} . On the contrary, if P_g is greater than P_r , the converter is in boost mode and $D2$ is controlled, such that the supercapacitor bank serves as a source to supply active power, which results in the decrease of its voltage V_{SC} . Therefore, by controlling the operating modes and duty ratios of the dc/dc converter, the ESS serves as either a source or a sink of active power to control the generated active power of the WTG. In Fig. 4, the reference signal P^*_g is generated by the high-layer WFSC.

and the duty ratio D2 of S2 in the boost mode is $D2 = 1 - D1$. In this paper, the nominal dc voltage ratio $V_{SC,n}/V_{dc,n}$ is

IV. WIND FARM FUZZY CONTROLLER and SUPERVISORY CONTROL

Fuzzy Logic controller

Fuzzy logic is a form of multi valued logic that can be taken from a fuzzy set theory. Fuzzy logic variables can have a truth logic between 0 and 1. Fuzzy logic is a good mean to control a system where there is no specific relation between input and output quantities. It has a simple rule based if-then approach to solve a control problem rather than modeling total system. This logic depends on operator's experience not on modeling of the system. Because of its usefulness in reducing complexity in mathematical models it is gaining more attention. In power system area fuzzy logic is used in stability studies, unit commitment, and reactive power control in distribution systems etc. fuzzy logic is made from fuzzification, knowledge rule base and defuzzification. Steps to design fuzzy based on wind speed: Choose the inputs to FLC: two inputs generator speed variation and speed derivative deviation used. Choose membership functions for inputs in fuzzy set notation. Triangular membership functions are used.

Defining knowledge rule base.

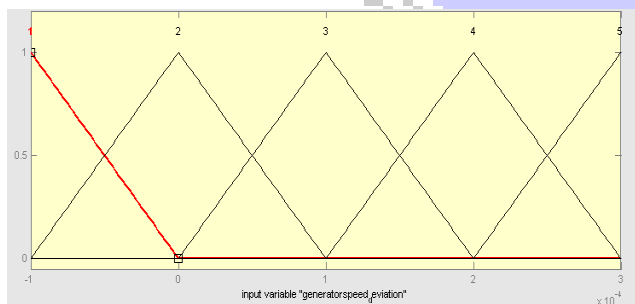


Fig.5(a) Wind speed deviation (Δe)

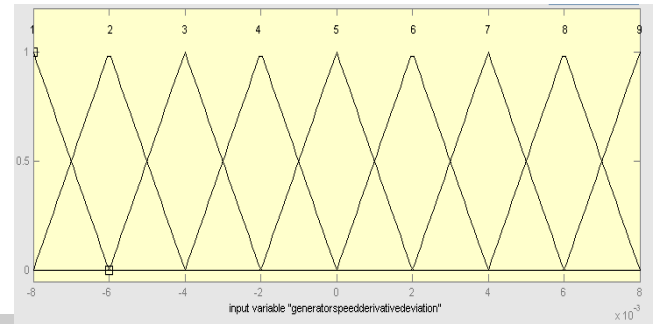


Fig.5(b) Grid voltage derivative deviation (Δe)

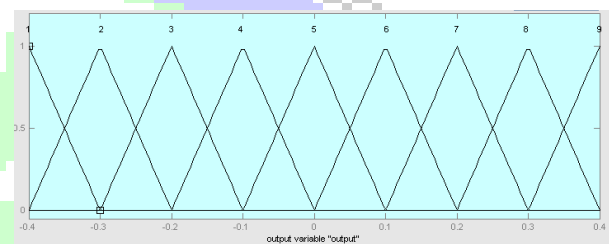


Fig.6(c) Fuzzy output

Fig 6(a,b&c). Membership functions of inputs and outputs. The objective of the WFSC is to generate the reference signals for the outer-loop power controllers of the RSC and GSC, the controller of the dc/dc converter, and the blade pitch controller of each WTG, according to the power demand from or the generation commitment to the grid operator. The implementation of the WFSC is described by the flowchart in Fig. 6, where P_d is the active power demand from or the generation commitment to the grid operator; v_{wi} and V_{essi} are the wind speed in meters per second and the voltage of the supercapacitor bank measured from WTG i ($i = 1, \dots, N$), respectively; and N is the number of WTGs in the wind farm. Based on v_{wi} , the optimal rotational speed

$\omega_{ti,opt}$ in radians per second of the wind turbine can be determined, which is proportional to the wind speed v_{wi} at a certain pitch angle β_i

$$\omega_{ti,opt} = k(\beta_i)v_{wi} \quad (3)$$

where k is a constant at a certain value of β_i . Then, the maximum mechanical power $P_{mi,max}$ that the wind turbine extracts from the wind can be calculated by the well-known wind turbine aerodynamic characteristics

$$P_{mi,max} = \frac{1}{2} \rho_i A_r v_{wi}^3 C_{pi}(\lambda_{i,opt}, \beta_i) \quad (4)$$

where ρ_i is the air density in kilograms per cubic meter; $A_r = \pi R^2$ is the area in square meters swept by the rotor blades with R being the blade length in meters; and C_{pi} is the power coefficient, which is a function of both tip-speed ratio λ_i and the blade pitch angle β_i , where λ_i is defined by

$$\lambda_i = \frac{\omega_{ti} R}{v_{wi}} \quad (5)$$

In (4), $\lambda_{i,opt}$ is the optimal tip-speed ratio when the wind turbine rotates with the optimal speed $\omega_{ti,opt}$ at the windspeed v_{wi} .

Given $P_{mi,max}$, the maximum active power $P_{ei,max}$ generated by the WTG can be estimated by taking into account the power losses of the WTG [14]

$$P_{ei,max} = P_{mi,max} - P_{Li} = P_{si,max} + P_{ri,max} \quad (6)$$

where P_{Li} is the total power losses of WTG i , which can be estimated by the method in [14]; $P_{si,max}$ and $P_{ri,max}$ are the maximum DFIG stator and rotor active powers of WTG i , respectively. In terms of the instantaneous variables in Fig. 1, the stator active power P_s can be written in a synchronously rotating dq reference frame [16] as follows:

$$P_s = \frac{3}{2} (v_{ds} i_{ds} + v_{qs} i_{qs}) \approx \frac{3}{2} [\omega_s L_m (i_{qs} i_{dr} - i_{ds} i_{qr}) + r_s (i_{ds}^2 + i_{qs}^2)] \quad (7)$$

where v_{ds} and v_{qs} are the d- and q-axis voltage components of the stator windings, respectively; i_{ds} and i_{qs} are the stator d- and q-axis current components, respectively; i_{dr} and i_{qr} are the rotor d- and q-axis current components, respectively; ω_s is the rotational speed of the synchronous reference frame; and r_s and L_m are the stator resistance and mutual inductance, respectively. Similarly, the rotor active power is calculated by

$$P_r = \frac{3}{2} (v_{dr} i_{dr} + v_{qr} i_{qr}) \approx \frac{3}{2} [-s \omega_s L_m (i_{qs} i_{dr} - i_{ds} i_{qr}) + r_r (i_{dr}^2 + i_{qr}^2)] \quad (8)$$

where v_{dr} and v_{qr} are the d- and q-axis voltage components of the rotor windings, respectively; s is the slip of the DFIG defined by

$$s = (\omega_s - \omega_r) / \omega_s \quad (9)$$

where ω_r is the DFIG rotor speed. (7) and (8) yield

$$s = -\frac{P_r - 3i_r^2 r_r}{P_s - 3i_s^2 r_s} \quad (10)$$

Where $i_s = \sqrt{i_{ds}^2 + i_{qs}^2}/2$ and $i_r = \sqrt{i_{dr}^2 + i_{qr}^2}/2$.

If neglecting the stator copper loss $3i_s^2 r_s$ and rotor copper loss $3i_r^2 r_r$ of the DFIG, the relationship between the stator and rotor active powers can be approximated by

$$P_r = -sP_s \quad (11)$$

According to (6) and (10) [or (11)], $P_{si,max}$ and $P_{ri,max}$ of each WTG can be determined. Then, the total maximum mechanical power $P_{m,max}$, DFIG output active power $P_{e,max}$, and stator active power $P_{s,max}$ of all WTGs in the wind farm can be calculated as

$$P_{m,max} = \sum_{i=1}^N P_{mi,max} \quad (12)$$

$$P_{e,max} = \sum_{i=1}^N P_{ei,max} \quad (13)$$

$$P_{s,max} = \sum_{i=1}^N P_{si,max} \quad (14)$$

In order to supply constant power P_d to the grid, the deviation $P_{ess,d}$ between the demand/commitment P_d and the maximum generation $P_{e,max}$ is the power that should be stored in or supplied from the ESSs of the WTGs

$$P_{ess,d} = P_{e,max} - P_d \quad (15)$$

On the other hand, the capability of each ESS to store or supply power depends on the capacitance C_{ess} and the voltage V_{essi} of the supercapacitor bank. During normal operation, V_{essi} must be maintained within the following range:

$$V_{i,min} < V_{essi} < V_{i,max} \quad (16)$$

where $V_{i,max}$ and $V_{i,min}$ are the maximum and minimum operating voltages of the supercapacitor bank, respectively. The maximum power $P_{essi,max}$ that can be exchanged between the supercapacitor bank and the DFIG dc link of WTG i can be determined by

$$P_{essi,max} = \pm C_{ess} V_{essi} \left| \frac{dV_{essi}}{dt} \right|_{max} \quad (17)$$

where $|dV_{essi}/dt|_{max}$ is the maximum rate of voltage variations of the supercapacitor bank, which is related to the current limits of the supercapacitor bank. In (17), the positive sign indicates storing energy, while the negative sign indicates supplying energy by the ESS. The calculation of $P_{essi,max}$ for each WTG is subjected to (16). Fig. 7 shows how to determine $P_{essi,max}$ for each WTG. If $P_{ess,d} > 0$, extra power needs to be stored in the ESSs. In this case, if $V_{essi} < V_{i,max}$, $P_{essi,max}$ is calculated by (17) and takes the positive sign; otherwise, the ESS cannot store any power and $P_{essi,max} = 0$. On the contrary, if $P_{ess,d} < 0$, active power needs to be supplied from the ESSs. In this case, if $V_{essi} > V_{i,min}$, $P_{essi,max}$ is calculated by (17) and takes the negative sign; otherwise,

the ESS cannot supply any power and $P_{essi,max} = 0$.

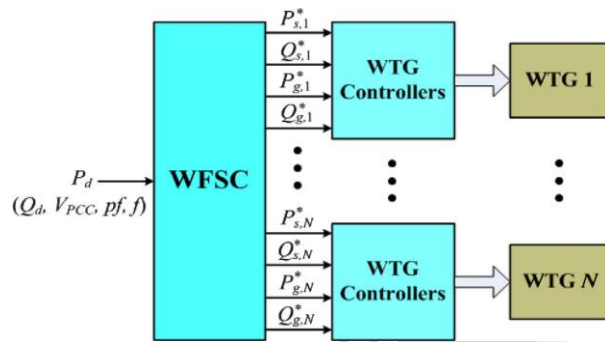


Fig. 7. Proposed two-layer CPC scheme for the wind farm.

As shown in Fig. 6, once $P_{essi,max}$ of each WTG is determined, the total maximum power $P_{ess,max}$ that can be exchanged between the supercapacitor bank and the DFIG dc link of all WTGs can be determined by

$$P_{ess,max} = \sum_{i=1}^N P_{essi,max} \quad (18)$$

Finally, depending on the relationship of $P_{ess,d}$ and $P_{ess,max}$, the reference signals P^*_{si} (see Fig. 2) and P^*_{gi} (see Fig. 4) of each WTG can be determined. Specifically, if $|P_{ess,d}| \leq |P_{ess,max}|$, P^*_{si} and P^*_{gi} can be determined directly, as shown in Fig. 6, where the partition coefficients a_i 's are calculated by

$$a_i = \frac{P_{r,max}}{P_{s,max} - P_{s,max}} \quad (19)$$

and the partition coefficients b_i 's are calculated by

$$b_i = \frac{P_{essi,max}}{P_{ess,max}} \quad (20)$$

The coefficients a_i and b_i have the following feature:

$$\sum_{i=1}^N a_i = 1 \quad \sum_{i=1}^N b_i = 1 \quad (21)$$

If $|P_{ess,d}| > |P_{ess,max}|$, depending on the sign of $P_{ess,d}$, P^*_{si} and P^*_{gi} can be determined, as shown in Fig. 6. If $P_{ess,d}$ is positive, the ESSs of the WTGs store active power, and the total active power generated by all DFIGs is P^*_{e} , which is less than $P_{e,max}$. Therefore, a scaling factor c is defined as follows

$$c = \frac{P^*_{e}}{P_{e,max}} \quad (22)$$

and P^*_{si} and P^*_{gi} can be determined by using the scaling factor. If $P_{ess,d}$ is negative, the ESSs of the WTGs supply active power, the RSC of each WTG is controlled to generate the maximum stator active power $P_{si,max}$, and the ESS of each WTG is controlled to generate active power of P^*_{gi} , where $P_{gi,max}$ is the maximum value of P_{gi} depending on the maximum power capacity of the GSC. Fig. 8 shows the block diagram of the proposed two-layer CPC scheme for the wind farm, where P_d is the active power demand from or commitment to the grid operator. In practice, the value of P_d should take into account the generation capability of the wind farm and should be subjected to the following limit:

$$P_d \leq \overline{P_{e,max}} \quad (23)$$

where $P_{e,max}$ is the average value of $P_{e,max}$ over the period that P_d will be constant and the value of $P_{e,max}$ during the period can be obtained from short-

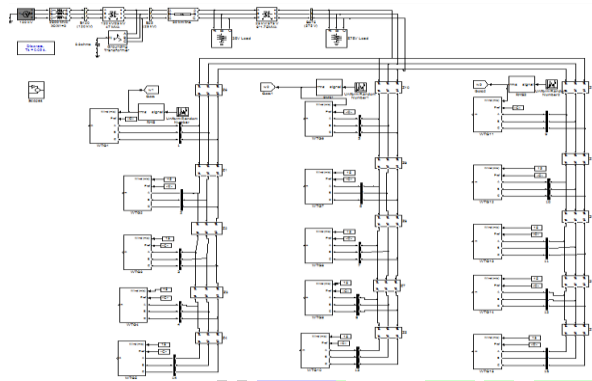


Fig. 9. Configuration of a wind farm equipped with 15 DFIG wind turbines connected to a power grid.

term wind power prediction [6]. This function allows the wind farm to be able to actively participate in automatic generation control, unit commitment, or frequency regulation of the grid, where the deviations between the available wind energy input and desired active power output are compensated by the ESSs. Under the condition of (23) and the ESS of a WTG has been fully filled up, then the power reference of the blade pitch controller in Fig. 5 is set at P_d by the WFSC to adjust the pitch angle to reduce the WTG output active power to P_d . Moreover, the implementation of the WFSC (Fig. 6) subject to (23) ensures that the use of the ESS does not need to increase the rating of the RSC or the GSC.

The reactive power references of the RSC (Fig. 2) and GSC (Fig. 3) controllers can be determined by controlling the power (pf) or the voltage (VPCC) at the point of common coupling (PCC) of the wind farm at the desired value or to supply a desired amount of reactive power as required by the grid operator. However, these issues are not in the scope of this paper. In this paper, the reactive power references of all RSC and GSC controllers are simply set as zero.

V. SIMULATION RESULTS

Simulation studies are carried out for a wind farm with 15 DFIG wind turbines (see Fig. 9) to verify the effectiveness of the proposed control scheme under various operating conditions. Each DFIG wind turbine (see Fig. 1) has a 3.6-MW power capacity. The total power capacity of the wind farm is 54 MW. Each DFIG wind turbine is connected to the internal network of the wind farm through a 4.16/34.5-kV voltage step-up transformer. The high-voltage terminals of all transformers in the wind farm are connected by 34.5-kV power cables to form the internal network of the wind farm. The entire wind farm is connected to the utility power grid through a 34.5/138-kV voltage step-up transformer at PCC to supply active and reactive powers of P and Q , respectively. In this paper, the power grid is represented by an infinite source. The ESS of each WTG is designed to continuously supply/store

20% of the DFIG rated power for approximately 60 s. Then, the total capacitance of the supercapacitor bank can be obtained from (1). The parameters of the WTG, the ESS, and the power network are listed in the Appendix. Some typical results are shown and discussed in this section.

A. CPC During Variable Wind Speed Conditions

Fig. 10 shows the wind speed profiles of WTG1 (vw1), WTG6 (vw6), and WTG11 (vw11). The wind speeds across the three WTGs vary in a range of ± 3 m/s around their mean value of 12 m/s. The variations of wind speed cause fluctuations of the electrical quantities of the WTGs. As shown in Fig. 11, if the wind farm is not equipped with any energy storage devices or the proposed CPC scheme, the wind speed variations in the wind farm result in significant fluctuations of the total output active power at the PCC. The wind farm power output deviates significantly from the active power demand or commitment. In future electric power grids where the penetration of wind power is high (e.g., 20%), such active power fluctuations can bring severe problems to grid operation.

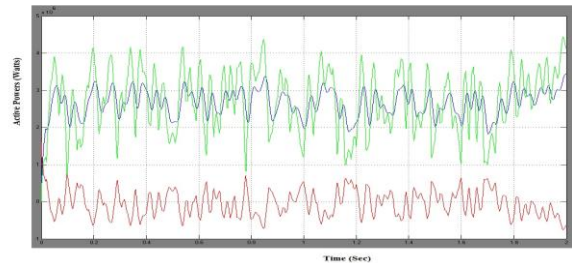


Fig. 11. Comparison of the wind farm power output (measured at PCC) and the constant power demand from or commitment to the grid operator: Without ESSs and the proposed CPC scheme.

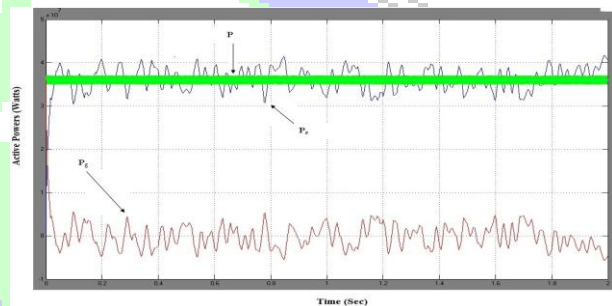


Fig. 12. Comparison of the wind farm power output (measured at PCC) and the constant power demand from or commitment to the grid operator: With ESSs and the proposed CPC scheme.

VI. CONCLUSION:

This paper has proposed a novel two-layer CPC scheme for a wind farm equipped with DFIG wind turbines. Each wind turbine is equipped with a supercapacitor-based ESS with FUZZY controller, which is connected to the dc link of the DFIG through a two-quadrant dc/dc converter. The ESS serves as either a source or a sink of active power to control the generated active power of the DFIG wind turbine with FUZZY. Each

individual DFIG wind turbine and its ESS are controlled by low-layer WTG controllers, which are coordinated by a high-layer WFSC to generate constant active power as required by or committed to the grid operator. Simulation studies have been carried out for a wind farm equipped with 15 DFIG wind turbines to verify the effectiveness of the proposed CPC scheme. Results have shown that the proposed CPC scheme enabled the wind farm to effectively participate in unit commitment and active power and frequency regulations of the grid with FUZZY controller. The proposed system and control scheme provides a solution to help achieve high levels of penetration of wind power into electric power grids.

REFERENCES:

[1] "Focus on 2030: EWEA aims for 22% of Europe's electricity by 2030," *Wind Directions*, pp. 25–34, Nov./Dec. 2006.

[2] 20% Wind Energy By 2030: Increasing Wind Energy's Contribution to U.S. Electricity Supply, U.S. Department of Energy, Jul. 2008.

[3] W. Qiao and R. G. Harley, "Grid connection requirements and solutions for DFIG wind turbines," in *Proc. IEEE Energy Conf.*, Atlanta, GA, Nov. 17–18, 2008, pp. 1–8.

[4] Wind Generation & Total Load in the BPA Balancing Authority: DOE Bonneville Power Administration, U.S. Department of Energy. [Online]. Available:

<http://www.transmission.bpa.gov/business/operations/Wind/default.aspx>

[5] R. Piwko, D. Osborn, R. Gramlich, G. Jordan, D. Hawkins, and K. Porter, "Wind energy delivery issues: Transmission planning and competitive electricity market operation," *IEEE Power Energy Mag.*, vol. 3, no. 6, pp. 47–56, Nov./Dec. 2005.

[6] L. Landberg, G. Giebel, H. A. Nielsen, T. Nielsen, and H. Madsen, "Short-term prediction—An overview," *Wind Energy*, vol. 6, no. 3, pp. 273–280, Jul./Sep. 2003.

[7] M. Milligan, B. Kirby, R. Gramlich, and M. Goggin, Impact of Electric Industry Structure on High Wind Penetration Potential, Nat. Renewable Energy Lab., Golden, CO, Tech. Rep. NREL/TP-550-46273. [Online]. Available: <http://www.nrel.gov/docs/fy09osti/46273.pdf>

[8] J. P. Barton and D. G. Infield, "Energy storage and its use with intermittent renewable energy," *IEEE Trans. Energy Convers.*, vol. 19, no. 2, pp. 441–448, Jun. 2004.

[9] D. Rastler, "Electric energy storage, an essential asset to the electric enterprise: Barriers and RD&D needs," California Energy Commission Staff Workshop Energy Storage Technol., Policies Needed Support California's RPS Goals 2020, Sacramento, CA, Apr. 2, 2009.